Archives of Environmental Protection
Vol. 50 no. 1 pp. 87–94

PL ISSN 2083-4772
DOI:10.24425/aep.2024.149435

Numerical model for simulating the hydraulic parameters of the aeration system ensuring equal oxygenation of the compost heap

Robert Sidełko[1]*, Dariusz Boruszko[2]

[1] Koszalin University of Technology, Poland
[2] Bialystok University of Technology, Poland

* Corresponding author's e-mail: robert.sidelko@tu.koszalin.pl

Keywords: composting, waste, mathematical modelling, aeration

Abstract: The aim of the work was to develop a mathematical model using equations of fluid mechanics that describe the dynamics of air flow in a part of the compost aerating system integrated with a stationary reactor. The results of the simulation show that adjusting the flow resistance along the entire length of the compost aerating duct, depending on the distance from the connection of the duct with the fan's pressure conduit pipe through gradually increasing the air outflow area by increasing the number of repeatable gaps, yields a uniform pressure distribution above the grate. The process parameters used for computation were relevant to composting a subscreen fraction separated from mixed municipal waste using 80 mm mesh screen (Fr<80 mm) under real conditions. Microsoft EXCEL 2010 software and STATISTICA version 13.3 by StatSoft were used for numerical and statistical analysis of the test results. The research results are presented in four tables and five figures and discussed in the text of the article. During tests performed in real conditions, various variants were tested for reactor filling level and air outflow active surfaces in subsequent grate parts (Fc (i)). It was found that the target waste layer thickness i.e. 3.0 m and Fc (i) changes, in accordance with the values of the developed model, result in a stable pressure distribution pd, amounting to 1506 Pa and 1495 Pa at the grate front and end part.

Introduction

Composting is a method of biological transformation of organic matter into a product, which, depending on the raw material quality, can be classified as organic fertilizer (Sadeghi et al. 2022) or stabilized compost (Vaverkova et al. 2020, Pączka et al. 2018, Klimek et al. 2018, Gałwa-Widera et al. 2016). Regardless of the final product, composting in biological reactors, unlike methane fermentation (Sidełko and Chmielińska-Bernacka 2013, Kisielewska et al. 2020), is an oxygen- consuming process requiring vigorous aeration. Unit mass ranges for oxygen supplied to composted material to ensure the correct course of the process were defined for three ranges: 2.6÷4.3 mg O_2/g o.m./h for low aeration, 6.1÷19.6 mg O_2/g o.m./h for medium aeration, and 21.8÷51.8 mg O_2/g o.m./h for high aeration, respectively (Epstain 1997). In terms of air volume at normal condition, the entire range for the above-indicated rates is 0.3÷5.4 m^3/kg o.m. over 24 hours. It can be concluded from available literature that in practice, the above parameter value falls within 0.6÷1.9 m^3/kg o.m./day range (Sidełko et al. 2011). Different optimum aeration rates have been reported in previous studies. Nguyen et al. (2022) found a delay in organic matter degradation with an aeration intensity below 13 ml O_2/min/kg w.s. of a mixture of rabbit food with sawdust as a bulking agent and commercial seeding material mixed in proportion 10:9:1 by weight. Sundberg and Jonsson (2008) studied the effect of aeration intensity on the composting of biodegradable waste from households. Three intensities of positive aeration were used: 10, 30 and 50 m^3 air/m^3 compost/h. The tests were carried out in industrial conditions using concrete bays. All bays achieved similar temperatures during low pH conditions, regardless of the aeration rate.

One of the largest biologically stabilized waste streams under aerobic conditions is the granulometric fraction Fr<80 mm, mechanically separated from mixed municipal waste (Bernat et al. 2022, Szymański et al. 2007). This fraction constitutes, on average, 50.6% of total mass of mixed waste (Jędrczak and Den Boer 2015). Test performed on waste supplied to a mechanical-biological transformation plant (MBT), which involved the analysis of its structure and physicochemical properties, revealed that Fr<80 mm contains, on average, 47.4% of biodegradable components, of which organic substances constitute 41.6% d.m. (Jędrczak and Den Boer 2015). Morphological composition of Fr<80 mm features a relatively high content of inert materials such as, among others, plastics, minerals, metals, and glass (Tab. 1).

The presence of the above-mentioned waste components in the entire mass of Fr<80 mm, totaling approximately 52%, has a beneficial impact on the composted mass structure, improving its key physical parameter, namely porosity (Zhou et al. 2022). However, in the case of stationary reactors filled with batch material, there is a risk of waste self-densification, causing porosity decrease from 40% to 10%, resulting in a five-fold increase of airflow resistance (Singley et al. 1982). According to the sources available, unit resistance of the bed formed of municipal waste, falls within 20÷1000 Pa/m range (Frederickson et al. 2013, Lelicińska-Serafin K. 2009).

The essence of efficient aeration lies in supplying oxygen in the same or possibly comparable volume to every place in the composted material, ensuring oxygen concentration in compost pores of 15÷20% (Nogueira da Silva et al. 2022). The element of the aeration installation that has a decisive impact on the even air outflow from the duct supplying air to the windrow should be a properly perforated grate covering the duct. The compost windrow aeration duct is integrated with the reactor floor and, apart from air supply, is also used to drain away surplus water. Air flows out from grate openings along its entire length directly into the composted mass, and then the post-process air flows into the space in which atmospheric pressure exists. Such solutions are common in the majority of composting techniques performed in static conditions with forced aeration available in the Polish market (Horstmann, Aknova, Sutco).

From a hydraulic perspective, the compost aeration installations in use are open systems, which means that the pressure above the compost layer is close to the atmospheric pressure. Therefore, ensuring uniform aeration of the compost covering the duct along its entire length requires pressure regulation or control in subsequent grate parts or sections. A similar issue is associated with mechanical air-supply installation where throttles equipped with electric drives are used to control flow of air. The flow rate values of the air-supply screens located in different compartments are controlled by measuring static pressure in relevant places of the installation (Yi Wang et al. 2022, Cui et al. 2020). On the other hand, in closed -system installations, such as in a tubular heat exchanger through which air flows, achieving a similar flow in exchanger sections connected in parallel with the air supply and discharge duct can be achieved using the so-called Tichelman's arrangement (Guohui 2017).

In the case of compost windrow aeration ducts, achieving uniform air outflow from the grate along the entire duct length can be challenging without proper surplus pressure choking. This necessitates sectional dimensioning of the grate's active surface covering subsequent, separated duct sections, especially when static pressure gradually decreases in the airflow direction. Currently, it is difficult to find solutions that guarantee uniform compost aeration when ducts located in the reactor floor are used. Although concrete grates used in practical solutions have properly profiled gaps or aerating nozzles, in most cases, the spacing and dimensions of these gaps, as well as aerating nozzles, indicate that their design was accomplished without applying hydraulic balancing principles (Horstmann, Aknova, Sutco).

This paper presents a mathematical model using fluid mechanics equations to describe the flow of fluids and gases in pressurized ducts, employing the Bernoulli's, Darcy-Weisbach's, and continuity of flow equations. The practical dimension of the developed model involves the creation of a computational algorithm, serving as a tool to design the air flow surface for air flowing through the grate covering subsequent sections of the duct supplying air to the composting process. Achieving uniform compost aeration, especially in the ducts of considerable length, which may reach up to 30 m, necessitates computation taking into account gradual pressure drop depending on the distance of a given section from the duct connection to the air supplying installation. This installation is equipped with radial fans capable of producing high nominal pressure of 3÷7 kPa.

Materials and methods

Process parameters used for computational purposes were relevant for composting a subscreen fraction in real conditions, separated from mixed municipal waste using 80 mm mesh screen (Fr<80 mm). The technical object in which measurements were taken during the developed model validation was Municipal Waste Processing Plant (MWPP) in Katowice, Poland. The composting technique employed at this plant involves the use of steel-reinforced concrete stationary reactors with ducts located in the reactor floor and in application of positive aeration. Each reactor has 4 aeration ducts of 28 m in length each. Such reactors are filled with Fr<80 mm batch material up to a target height 3.0 m and tightly closed after filling. During the tests performed to verify the developed model, pressure above the duct covering the air-supply grate was measured at three points: at the front part (p_f), in the middle (p_m), and at the duct end (p_{end}). PC-28 Aplisens pressure sensors (0÷2.5 kPa), monitoring static pressure, were placed in a perforated metal casing directly on the aerating grate at points relevant for the front, middle and end sections.

For statistical analysis of test results, Microsoft EXCEL 2010 software and STATISTICA version 13.3 by StatSoft were used. The scope of applied statistical tools comprised the nonlinear regression issues and selected statistics available in the Basic Statistics and tables module of STATISTICA.

Table 1. Composition of the Fr<80 mm from 20 MBT installations (Jędrczak and Den Boer 2015).

Components	Values		
	average	st.dev.	median
Organic no.1[1]	12.70	11.5	8.6
Organic no.2[2]	34.7	11.3	35.9
Wood	0.6	0.9	0.3
Plastics	5.7	3.7	5.1
Glass	11.5	5.5	9.7
Textilies	0.6	0.5	0.6
Metals	1.3	1	1
Inert	20.7	16.7	17.1
Other[3]	12.20	-	-

[1]- food, [2]- parks, gardens, [3] - composites, electronics, batteries

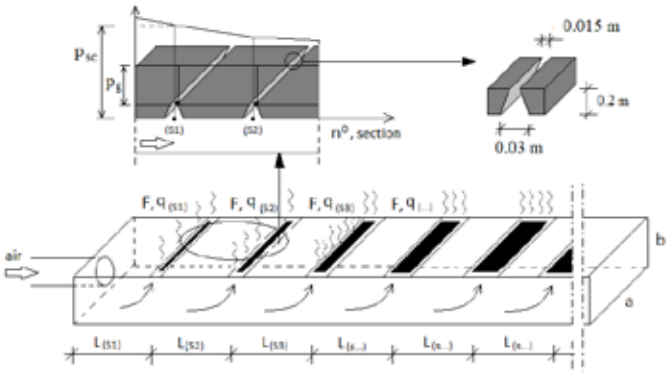

Figure 1. Diagram of the air supply duct with the gap detail.

Model

For numerical computations, a concrete structure of an aeration duct featuring a rectangular cross-section was adopted. Ducts of such type are used for air supply to biological material filling stationary reactors as well material collected and formed as a compost windrow covered with a vapor-permeable membrane or a coverless windrow kept in a separate production hall (Rudnik 2019). Depending on the technique, two methods of active aeration consisting of air flow from the grate covering the duct to the windrow, and vice versa, i.e., positive and negative aeration, are applied (Wang et al. 2018). An aeration duct diagram comprising particular physical values is shown in Figure 1. In subsequent sections: s (1), s (2), s (3),…,s (n), thick lines in the place of aeration duct covering grates symbolize active surfaces of air flow from the duct via the grate to compost according to the following principle:

$$\sum F_{g\,(1)} < \sum F_{g\,(2)} < \sum F_{g\,(3)} < \ldots < \sum F_{g\,(n)} \qquad (1)$$

where ΣFg (n) - total area of gaps in a given section.

Bottom index - g defines the gap constituting a principal element of the concrete grate. Total surface $\sum F_g$ is a product of the gap unit surface and number of gaps. Single gap featuring trapezoid cross-section with the upper and bottom widths of the base being 0.015 m and 0.03 m respectively and a length of 0.25 m long (Fig.1).

In contrast to the gradually increasing surface of air outflowing from the grate (1), the static pressure in the duct, according to the direction of flow in subsequent sections, systematically drops in the following way:

$$p_{sc\,(1)} > p_{sc\,(2)} > p_{sc\,(3)} > \ldots > p_{sc\,(n)} \qquad (2)$$

According to the energy conservation law, description of the real fluid dynamics in an enclosed duct is described by Bernoulie equation as follows:

$$\frac{v^2}{2g} + \frac{p}{\gamma} + \sum \Delta p = const \qquad (3)$$

The particular terms in equation (3) have linear dimension. Energy loss originates from the resistance of flow of fluid, whether it be liquid or gas, including air (ΣΔp), in straight duct sections. This loss results from changes of the flow direction, variations in cross-section area, and the utilization of flow control devices.

Pressure losses due to linear and local resistance, depending on air flow speed (v) can been described by the following equations:

$$\Delta p_l = \lambda \frac{v^2}{2g} \frac{l}{D} \qquad (4)$$

$$\Delta p_m = \zeta \frac{v^2}{2g} \qquad (5)$$

where*:* λ, ξ are the linear and local resistance coefficients, respectively.

Equations (3), (4) and (5) along with the flow continuity equation in the following form:

$$q = F \cdot v = const \qquad (6)$$

where v is the speed of air flow in the area with cross-section F, form the basis for the developed mathematical model. The structure of the model was based on the following assumptions:

(I) The volume of air flowing from the grate to the compost (q_g) – positive aeration, remains constant in each section;

(II) The aeration duct is uniformly covered by a compost leyer along the entire length ;

(III) The static pressure at the outflow from grates (p_g) remains constant along the entire duct length $(\sum_1^n l_s)$;

(IV) A gradual static pressure drop (Δp_{sc}) along the duct axis occurs in accordance with the flow direction, based on the principle described in equation (2) (Fig.1);

(V) Pressure surplus choking during air flow through the grate results from the flow resistance through a single gap (Δp_g) through which such flow is proportion to the number of gaps (quantity) making the grate's active surface relevant for the given section;

(VI) Active surfaces of the grates through which air flows in subsequent sections change in accordance with principle described in equation (1);

(VII) Flow resistance for particular installation parts was determined in the following way:

– The concrete aeration duct generates linear resistance in the sections, the values of which were computed as per (4) for λ=0.04 (Lubczyńska 2017) which allows to determine an equation for the function describing $\Delta pc=f(q)$ relationship - duct hydraulic characteristic, in the following form:

$$\Delta p_c = 0.0077 - 0{,}0308 \cdot q + 22{,}154 \cdot q \cdot q \qquad (7)$$

– The grate has gaps (Fig. 1.) each of which features local resistance factor (Lubczyńska 2017), whereas the pressure loss computed from equation (5) for a determined flow allows us to determine the equation for the function describing relationship - hydraulic characteristic of a single gap in the following form:

$$\Delta p_g = 0.001 - 0{,}0268 \cdot q + 207350 \cdot q \cdot q \qquad (8)$$

where q is the flow rate.

(VIII) The static pressure directly above the grate in each section has an equivalent value of a product of compost layer thickness and unit resistance:

$$p_{d\,(n)} = \Delta p_{uc} \cdot H = \text{const} \qquad (9)$$

where $p_{d\,(n)}$ (static pressure directly above the grate), p_{uc} (unit resistance of air flowing through the compost bed, H (compost layer thickness).

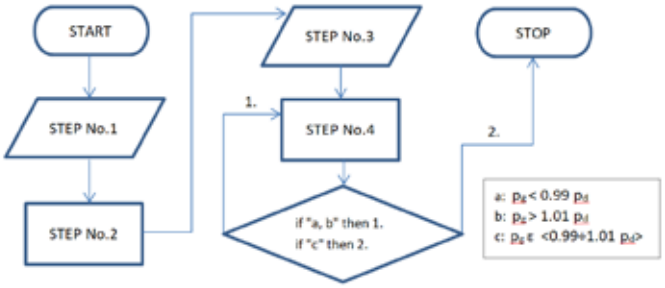

Figure 2. A block diagram of a computational algorithm.

(IX) The unit resistance of air flowing through the compost bed is Δp_{uc}= 500 Pa/m;

(X) The pressure above the compost bed is equal to the atmospheric pressure (p_{atm}).

Using (1÷6) relationships and defined boundary conditions (i÷x), a computational algorithm in the form of a Microsoft Excel Office 2010 spreadsheet was developed.

Algorithm

The computational algorithm consists of 5 steps (Tab. 2): entering data used in computation of concrete duct hydraulic parameters, step No 1, computation of air flow in the duct as well as the drop of static pressure in particular sections, and development of the duct hydraulic characteristic – step No 2, entering the data pertaining to the design of a single gap through which air flows from the duct to the compost located in the duct covering grate – Step No 3, computation of substitute parameters of a rectangular cross-section gap along with development of the gap hydraulic characteristic equation, fixing (first iteration) the number of gaps in the grate covering each duct section (ING - Increasing Number of Gaps), as well as computation of the pressure drop for air flowing through the gaps in subsequent sections covering grates – step No 4, verification of the computed pressure drop value for the set flow through the gap in a given section based on a criterion of admissible deviation from the criterial value of the adopted disposable pressure above the grate (±0.5%) and the optional change of the number of gaps for a given section (second iteration) – step No 5. The computational algorithm diagram is presented in Figure 2.

The key step is No 4. The static pressure surplus at the point of duct covered by a grate in a given section ($p_{sc\,(n)}$) with relation to the next section ($p_{sc\,(n+1)}$) is obtained by reducing the number of gaps. In such a case, compliance with condition (i) must result in increased flow through a single gap, which increases the local pressure drop (5) finally by the following values:

$$qnty._{(1)}.q_{g\,(1)} = qnty._{(2)}.q_{g\,(2)} = \ldots = qnty._{(n)}.q_{g\,(n)} \qquad (10)$$

Knowing the single gap characteristic equation (8) and arbitrarily fixed gap numbers in those grate places that are relevant for given sections, the flow of air in subsequent single gaps is computed in accordance with the following rule:

$$qnty._{(1)}.q_{g\,(1)} = qnty._{(2)}.q_{g\,(2)} = \ldots = qnty._{(n)}.q_{g\,(n)} \qquad (11)$$

where $$q_{g\,(1)} > q_{g\,(2)} > \ldots > q_{g\,(n)} \qquad (11a)$$

$$qnty._{(1)} < qnty._{(2)} < \ldots < qnty._{(n)} \qquad (11b)$$

The transformation of equation (10) leads to the following formula:

$$q_{g(n-1)} = qnty._{(n)} \frac{q_{g(n)}}{qnty._{(n-1)}} \qquad (12)$$

Computation shall commence from the end section and then, step by step, for subsequent sections in the direction opposite to the air flow in the duct.

Results

The algorithm operation required the predefinition of equations for the functions rendering hydraulic characteristics of the aeration duct (7) and the gap through which air is supplied to compost (8). Both equations were developed in steps No 2 and No 4 of the developed algorithm, respectively, and the result is presented in Figure 3.

Striving to provide uniform air outflow along the entire duct length, there is a necessity to adjust surplus pressure by altering the number of gaps in subsequent parts of the grate covering the aeration duct. Fixing the initial number of ducts, an assumption was made that gradual reduction of their numbers will result in unit flow decrease and, consequently, in the reduction of pressure drop of air flowing through the gaps in subsequent sections. In the first iteration, the ex ante adopted number of gaps was gradually reduced for every other section by two gaps assuming the initial value qnt. (ING)= 14. The result of simulation that was performed using the developed model is presented in Table3.

Table 2. Description of the scope the next steps in the evaluated algorithm.

Level	Step				
	no.1	no.2	no.3	no.4	no.5
1	total flow qt , m³/s	duct diameter (equivalent) F_c, m	gap_parameters	gap's characteristics Δpg=f (q)	decision
2	number of sections n, (-)	flow in each section qs (no.), m³/s		gap's outflow in each sections $q_{g\,(no.)}$, m³/s	
3	duct length l, m	air speed in sections $v_{s\,(no.)}$, m/s		quantity of gaps in each sections, (qnty.)	
4	duct dimention a/b, m	pressure loss in sections ∆p, Pa		gap's outlet air pressure, Pa	
5	length of one sect. $l_{s\,(no.)}$, m	static pressure in sections ps, Pa		-	
6	disposal pressure over gaps pd, Pa	duct's characteristics Δpc=f (q)		-	

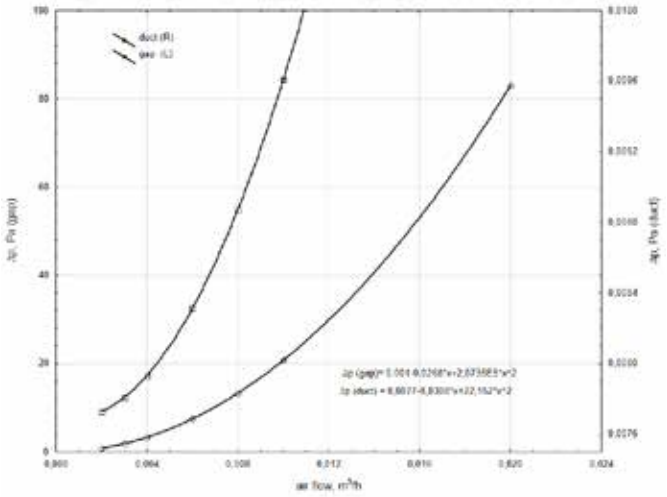

Figure 3. Hydraulic characteristics of the aeration duct and gaps.

The pressure values obtained at air outlets from the grate along the entire duct length fluctuate around 1500 Pa, except for first two cases – sections (Tab. 3). The static pressure difference at the outflow of the grate between the duct front and end part appeared to be approximately 70 Pa. The computed p_g value above the grate in the front duct part, amounting to 1430 Pa versus the required 1500 Pa, fails to guarantee proper air flow, and consequently, the required oxygenation of compost. The results obtained were verified by computation of the relative error value determining the difference between the computed pressure value p_g and set value p_d, taking into account the arbitrarily applied admissible deviation ±1% i.e. <1485 Pa÷1515 Pa>. The above error was defined in the following way:

$$\text{error} = \pm (1500\text{-}p_g) \cdot 100/1500 \qquad (13)$$

It was found that the biggest error fluctuation occurred in the front sections of the grate covering the aeration duct. The error value (13) exceeded the admissible value in two cases related to sections No 1 & No 2 and amounted to 4.7 and 5.4, respectively (Tab. 3). In the second iteration, in the majority of cases, corrections of the number of gaps were made to ensure that the error value (13) falls within the admissible limits. Error dispersion before and after gap number correction is presented in Figure 4.

Striving for uniform compost aeration along the entire windrow length, it was assumed, as a consequence of condition (i), that air flow in subsequent sections will gradually decrease by a constant value equal to the volume of air outflowing through the subsequent grate parts. It should be underlined that the element stabilizing pressure above the grate, a constant value of which assures uniform air flow through the uniform compost windrow, is the number of gaps in a given part of the grate. The adopted boundary conditions (i÷x) indicate that the results generated by the algorithm were obtained for the set conditions. Therefore, during the operation of the entire installation, its particular parts must not change, in particular, the thickness of the compost layer, the target value of which amounts to 3.0 m. In the event when the composted waste (Fr<80 mm) windrow height is different form the set value, the hydraulic characteristic of the windrow changes, and

Table 3. Result of the model simulation for a 28 m long duct.

section					gap									
					calculated					after correction				
No.	q, m3/s	v, m/s	Δp, Pa	ps, Pa	qnty. (ING)	q, m3/s	Δp, Pa	pg, Pa	error1	qnty. (10)	q, m3/s	Δp, Pa	pg, Pa	error2
1	0.69	8.5	10.67	1557.9	2	0.025	127.66	1430.2	4.7	3	0.017	56.69	1501.2	-0.1
2	0.64	7.9	9.20	1547.2	2	0.025	127.66	1419.5	5.4	3	0.017	56.69	1490.5	0.6
3	0.60	7.3	7.84	1538.0	4	0.012	31.90	1506.1	-0.4	4	0.012	31.89	1506.1	-0.4
4	0.55	6.7	6.59	1530.2	4	0.012	31.90	1498.3	0.1	5	0.010	20.41	1509.7	-0.6
5	0.50	6.1	5.44	1523.6	6	0.008	14.17	1509.4	-0.6	5	0.010	20.41	1503.2	-0.2
6	0.45	5.4	4.41	1518.1	6	0.008	14.17	1503.9	-0.3	6	0.008	14.17	1503.9	-0.3
7	0.40	4.8	3.48	1513.7	8	0.006	7.97	1505.7	-0.4	6	0.008	14.17	1499.5	0.0
8	0.35	4.2	2.67	1510.2	8	0.006	7.97	1502.3	-0.2	6	0.008	14.17	1496.1	0.3
9	0.30	3.6	1.96	1507.6	10	0.005	5.10	1502.5	-0.2	8	0.006	7.97	1499.6	0.0
10	0.25	3.0	1.36	1505.6	10	0.005	5.10	1500.5	0.0	8	0.006	7.97	1497.6	0.2
11	0.20	2.4	0.87	1504.2	12	0.004	3.54	1500.7	0.0	8	0.006	7.97	1496.3	0.2
12	0.15	1.8	0.49	1503.4	12	0.004	3.54	1499.8	0.0	8	0.006	7.97	1495.4	0.3
13	0.10	1.2	0.22	1502.9	14	0.004	2.60	1500.3	0.0	8	0.006	7.97	1494.9	0.3
14	0.05	0.6	0.05	1502.7	14	0.004	2.60	1500.1	0.0	8	0.006	7.97	1494.7	0.4

* values changed manually

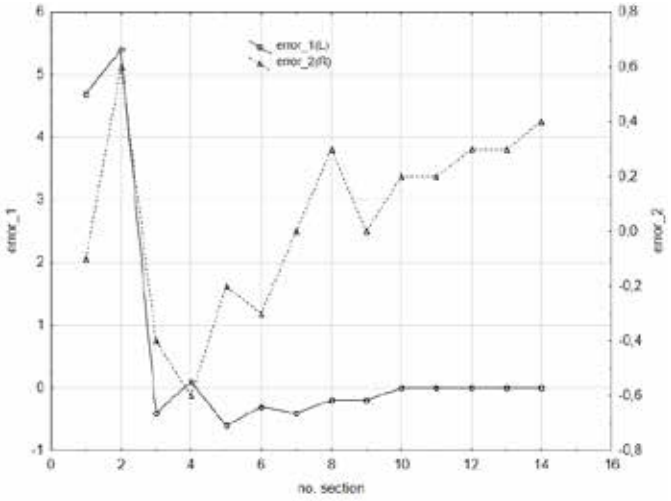

Figure 4. The dispersion of the corrected pg values in relation to the required pressure p_d.

consequently, the so-called substitute characteristic of the entire installation also changes (Ross 1995).

For example, the reduction of windrow height results in the flattening of the bed characteristic and shifting of the installation/fan cooperation point (Lanzerstorfer et al. 2016). The fan flow rate increases, and dynamic pressure goes up. The system strives to arrive at a hydraulic equilibrium condition in which the distribution of pressures on grate outlets will differ from the expected one. Such a situation was observed during the tests performed in industrial conditions associated with the validation of the developed model.

Model validation

In accordance with the composting technique applied in ZPOK, the flow rate of air supplied to a single reactor equipped with four aeration ducts amounts to approximately 2500 m^3/h/duct.

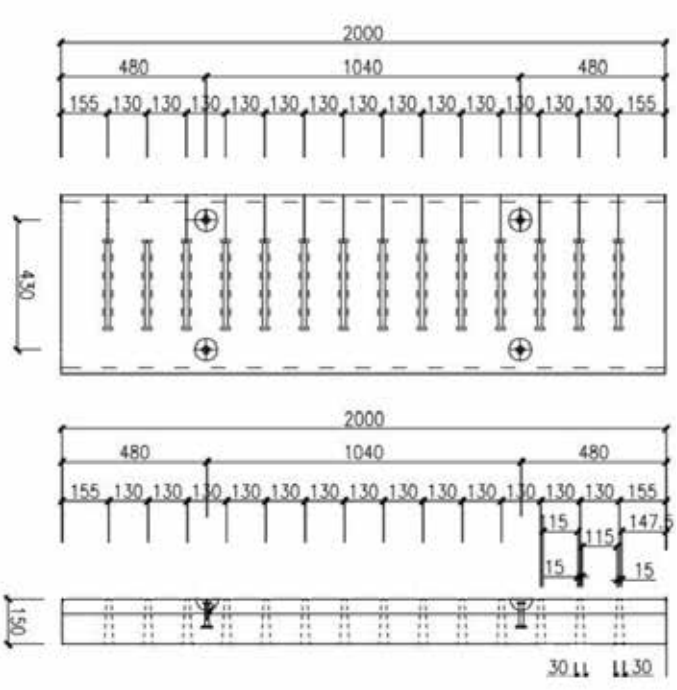

Figure 5. Construction of a concrete grate covering the aeration duct.

The concrete grate covering the duct is provided with gaps featuring the spacing. The shape and dimensions are presented in Figure 5.

The tests were performed for four variants: (a) empty reactor and all gaps opened; (b) empty reactor and some of the gaps opened – after correction, in particular sections as per data provided in Table 2; (c) all gaps opened and the reactor filled with target layer of the composted material (Fr<80 mm featuring thickness of 3 m); and (d) some of the gaps opened – after correction with reactor filled as in variant (c).

As in the two last variants, the waste bed introduced extra air flow resistance, thereby altering the substitute characteristic of the entire installation. In comparison to variants (a) and (b), fan operation parameters were adjusted to achieve an air flow per single duct in the reactor close to 2500 m^3/h, similarly to first two variants.

Comparing the results of pressure measurements for variants (c) and (d), it can be noted that for the adopted conditions, i.e., resistance of air flow through compost (ix) and target bed thickness, the value of the disposable pressure along the entire grate length is comparable (Tab. 4). This is likely a result of high fan compression originating from the excessive unit resistance values of the compost layer adopted at the industrial installation design stage. Tests performed by applying waste (Fr<80 mm) filled columns (Sidełko et al. 2019) have shown that the bed unit resistance during a 19-day experiment, at a comparable hydraulic load amounting to 60 m^3/m^2/h, increased to a maximum of approximately 200 Pa/m. Due to the considerably lower pressure drop during air flow through compost originating from excessive unit resistance - 500 Pa/m, the fan operating point coordinates changed; this originated from the intersection of its characteristic and the less inclined characteristic of the installation. This causes an increase in the flow rate above the required value, thus necessitating fan speed correction and a decrease in its pressure - compression.

The lower fan compression in variants (a) and (b) compared to higher compression in variants (c) and (b) causes relatively higher air flow in the front grate parts, leading to a quicker pressure drop in the duct down to values causing only minimal air outflow in further parts of the grate. Therefore, the fan compression factor is of key importance for stabilizing air outflow through the grate, the volume of which should be optimal, considering the cost of the so-called contracted power. At the same time, it should be stated that the application of variable air outflow surface along the entire grate length in low pressure conditions of the duct provides a beneficial

Table 4. Pressure values at different places above the grate for four variants.

Variant	Preassure, Pa			pend, (% pf)
	pf	pm	pend	
(a)	55	11	1	1.8
(b)	65	21	10	15.4
(c)	1565	1511	1488	95.1
(d)	1506	1496	1495	99.3

distribution of the volume of air flowing through the grate. This is proved by the fact that the pressure above the grate in the duct end part in variant (b) reached 15.4% of the pressure value at the grate front part, compared to 1.8% in variant (a).

Conclusion

The results obtained in real conditions indicate that the developed model allows for correct design of the perforation of the grate responsible for uniform compost aeration, as evidenced by the pressure values measured for variant (d) during the validation (Tab. 4). Comparing the pressure measurement results for variant (c), which involved the use of a grate with the same number of gaps along the entire duct length, with variant (d), in which the number of gaps gradually increased with distance from air supply pipe inlet, it was found that the grate made in accordance with model computations provides pressure distribution along the entire grate length close to the assumed level, i.e., 1500 Pa. At the same time, comparing the results obtained for variants (a) and (b), it is evident that if the reactor is not filled, the grate with variable perforation more effectively compensates the pressure drop along the entire duct length. The analysis indicates that the system gradually reaches a comparable pressure value at the outlet from the grate along its entire length as long as the compost layer thickness reaches the set value, i.e., 3.0 m.

References

Bernat, K., Kulikowska D., Wojnowska-Baryła, I. & Kamińska A. (2022). Can the biological stage of a mechanical biological treatment plant that is designed for mixed municipal solid waste be successfully utilized for effective composting of selectively collected biowaste, *Waste Management*, 149, pp. 291-301. DOI:10.1016/j.wasman.2022.06.025

Cui, C., Zhang, X. & Cai W. (2020). An energy-saving oriented air balancing method for demand controlled ventilation systems with branch and black-box model, *Appl. Energy*, 264, 11473. DOI:10.1016/j.apenergy.2020.114734

Frederickson, J., Boardman, C.P., Gladding, T.L., Simpson, A.E., Howell G. & Sgouridis, F. (2013). Biofilter performance and operation as related to commercial composting. US Environment Agency 2013.

Gałwa-Widera, M. & Kwarciak-Kozłowska, A. (2016). Methods for elimination of odor in the composting process, Rocznik Ochrona Środowiska, 18, pp. 850-860.

Guohui, G. (2017). Dynamic thermal simulation of horizontal ground heat exchangers for renewable heating and ventilation of buildings, *Renewable Energy*, 103, pp. 361-371. DOI:10.1016/j.renene.2016.11.052

https://www.horstmann.pl

https://www.aknova.pl

https://www.sutco.pl

Jędrczak, A. & Den Boer, E. (2015). Final report of the 3rd stage of an expert opinion aimed at conducting waste tests in 20 installations for mechanical-biological waste treatment. https://sdr.gdos.gov.pl/Documents/GO/Ekspertyzy.

Kisielewska, M., Dębowski, M. & Zieliński, M. (2020). Comparison of biogas production from anaerobic digestion of microalgae species belonged to various taxonomic groups. *Archives of Environmental Protection*, vol. 46, pp. 33-40. DOI:10.24425/aep.2020.132523

Klimek, A., Rolbiecki, S. & Rolbiecki R. (2018). Effects of mulching with forest litter and compost made of sewage sludge on the presence of oribatida as bioindicators of soil revitalization in larch and pine in-ground forest nurseries, *Rocznik Ochrona* Środowiska, 20, pp. 681-696.

Lanzerstorfer, Ch., Neder, F. & Schmied, R. (2016). Constant design air flow industrial ventilation systems with regenerative dust filters: Economic comparison of fan speed-controlled air damper controlled and uncontrolled operation, *Energy and Buildings*, 128, pp. 503–510. DOI:10.1016/j.enbuild.2016.07.032

Lubczyńska, U. (2017). Applied hydraulic in environmental engineering. Publishing House, Kielce University of Technology, 2017.

Nguyen, T.P., Koyama, M. & Nakasaki, K. (2022). Effects of oxygen supply rate on organic matter decomposition and microbial communities during composting in a controlled lab-scale composting system, *Waste Management*, Vol. 153, pp. 275-282. DOI:10.1016/j.wasman.2022.09.004

Nogueira Da Silva Vilela, R., Amorim Orrico, C.A., Previdelli Orrico Junior, M.A., Aspilcueta Borquis, R.R., Dias de Oliveira, M.T.J., De Avila M. R., Torres dos Santos, F. & Viana Leite, B.K. (2022). Effects of aeration and season on the composting of slaughter house waste, *Environmental Technol. & Innov*, 27, 102505. DOI:10.1016/j.eti.2022.102505

Pączka, G., Garczyńska, M., Mazur-Pączka, A., Podolak, A., Szura, R., Skoczko, I. & Kostecka, J. (2018). Vermicomposting of sugar beet pulps using Eisenia Fetida (sav.) earthworms, *Rocznik Ochrona* Środowiska, 20, pp. 588-601.

Ross, H. (1995). Hydraulik der wasserheizung Oldenbourg, Verlag GmbH, Monachium 1995. Rudnik E. (2019). Chapter 5 - Composting methods and legislation, Compostable Polymer Materials 2.nd Edition, pp. 127-161. DOI:10.1016/b978-0-08-099438-3.00005-7

Sadeghi, S., Nikaeen, M., Mohammadi, F., Nafez, A.H., Gholipour, S., Shamsizadeh, Z. & Hadi, M. (2022). Microbial characteristics of municipal solid waste compost: Occupational and public health risks from surface applied compost, *Waste Management*, 144, pp.98-105. DOI:10.1016/j.wasman.2022.03.012

Sidełko, R., Janowska, B., Szymański, K., Mostowik, N. & Głowacka, A. (2019). Advanced methods to calculation of pressure drop during aeration in composting process, *Science of the Total Environment*, 674, pp. 19-25. DOI:10.1016/j.scitotenv.2019.04.155

Sidełko, R., Seweryn, K. & Walendzik, B. (2011). Optimization of Composting Process in Real Conditions, *Rocznik Ochrona* Środowiska, 13, pp. 681-691.

Sidełko, R. & Chmielinska-Bernacka, A. (2013). Application of Compact Reactor for Methane Fermentation of Municipal Waste, *Rocznik Ochrona* Środowiska, 15, pp. 683-693.

Singley, M.E., Higgins, A.J. & Frumkin-Rosengaus, M. (1982). Sludge composting and utilization- A design and operating manual, New Jersy Arg. Expt. Sta., Rutgers Utility, 1982.

Sundberg, C. & Jönsson, H. (2008). Higher pH and faster decomposition in biowaste composting by increased aeration, *Waste Management*, Vol. 28, pp. 518-526. DOI:10.1016/j.wasman.2007.01.011

Szymański, K., Janowska, B., Sidełko, R. & Siebielska, I. (2007). Monitoring of waste landfills, VIII National Polish Scientific

Conference on Complex and Detailed Problems of Environmental Engineering, Issue 23, pp. 75-133.

Vaverkova, M.D., Elbl, J., Voberkova, S., Koda, E., Adamcova, D., Gusiatin, Z.M., Abd, Al Rahman, Radziemska, M. & Mazur, Z. (2020). Composting versus mechanical–biological treatment: Does it really make a difference in the final product parameters and maturity, *Waste Management*, 106, pp. 173-183. DOI:10.1016/j.wasman.2020.03.030

Yi, W., Ran, G. Li, A., Zhiguo, G., Ni, Q., Yang, Y., Liu, B. & Du, Y. (2022). Air balancing method of multibranch ventilation systems under the condition of nonfully developed Flow, *Boulding and Environment*, 223. DOI:10.1016/j.buildenv.2022.109468

Wang, X., Bai, Z., Yao, Y., Gao, B., Chadwick, D., Chen, Q., Hu, Ch. & Ma, L. (2018). Composting with negative pressure aeration for the mitigation of ammonia emissions and global warming potential, *J. of Cleaner Production*, 195 (10), pp. 448-557. DOI:10.1016/j.jclepro.2018.05.146

Zhou, Y., Xiao, R., Klammsteiner, T., Kong, X., Yan, B., Mihai, F.C., Liu, T., Zhang, Z. & Awasthi, K.M. (2022). Recent trends and advances in composting and vermicomposting technologies: A review, *Bioresources Technology*, 360, 127591. DOI:10.1016/j.biortech.2022.127591

Model numeryczny do symulacji parametrów hydraulicznych układu napowietrzania zapewniającego równomierne natlenienie pryzmy kompostowej

Streszczenie. Celem pracy było opracowanie modelu matematycznego wykorzystującego równania mechaniki płynów, które opisują dynamikę przepływu powietrza w części instalacji napowietrzającej kompost zintegrowanej z reaktorem stacjonarnym. Wyniki przeprowadzonej symulacji pozwalają stwierdzić, że regulacja oporów przepływu na całej długości kanału napowietrzającego kompost w zależności od odległości od połączenia kanału z przewodem ciśnieniowym wentylatora poprzez stopniowe zwiększanie powierzchni wypływu powietrza poprzez zwiększanie liczby powtarzalnych szczelin, zapewnia równomierny rozkład ciśnienia nad rusztem. Parametry procesu przyjęte do celów obliczeniowych były odpowiednie dla kompostowania frakcji podsitowej w warunkach rzeczywistych wydzielonej ze zmieszanych odpadów komunalnych za pomocą sita o oczkach 80 mm (Fr<80 mm). Do analizy numerycznej i statystycznej wyników badań wykorzystano oprogramowanie Microsoft EXCEL 2010 firmy oraz STATISTICA firmy StatSoft w wersji 13.3. Wyniki badań przedstawiono w czterech tabelach i pięciu rysunkach oraz omówiono w tekście artykułu. Wyniki uzyskane w warunkach rzeczywistych wskazują, że opracowany model pozwala na prawidłowe zaprojektowanie perforacji kraty odpowiadającej za równomierne napowietrzenie kompostu. W trakcie badań przeprowadzonych w warunkach rzeczywistych, gdy badano różne warianty stopnia napełnienia reaktora i powierzchni czynnych wypływu powietrza w kolejnych częściach rusztu (Fc (i)) stwierdzono, że docelowa grubość warstwy odpadów tj. 3,0 m oraz zmiany Fc (i), zgodnie z wartościami opracowanego modelu, skutkują stabilnym rozkładem ciśnień pd wynoszącym 1506 Pa i 1495 Pa w części czołowej i końcowej kraty.